Thin Solid Films 710 (2020) 138266

Contents lists available at ScienceDirect

Thin Solid Films

journal homepage: www.elsevier.com/locate/tsf

A green, low-cost method to prepare GaN films by plasma enhanced chemical vapor deposition

Qi Liang, Ru-Zhi Wang*, Meng-Qi Yang, Yang Ding, Chang-Hao Wang

College of Materials Science and Engineering, key Laboratory of Advanced Functional Materials, Education Ministry of China, Beijing University of Technology, Beijing 100124, China

ARTICLE INFO

Keywords:
Gallium nitride
Thin films
Plasma enhanced chemical vapor deposition method
Growth mechanism
Non-toxic raw materials
Photoresponsivity
Photoelectric devices

ABSTRACT

In this study, the GaN films have been prepared by a green and low-cost plasma enhanced chemical vapor deposition (PECVD)method on Al_2O_3 substrate, along with Ga_2O_3 and N_2 as gallium source and nitrogen sources, respectively. The results show that the oxygen content in the GaN films is significantly influenced by the reaction temperature and N_2 flow rate. The uniform and high crystallinity GaN films were obtained at 950 °C with N_2 flow rate 150 sccm, which was also proved by high- resolution transmission electron microscopy (HRTEM) analysis. It is found that the high energy nitrogen plasma and additive graphite play vital role in the growth of the high-quality GaN films; and the graphite, used as reductive agent, avoided the unfavorable effect caused by the hydrogen radicals, thus, contributing to the GaN nucleation. Moreover, the photoresponsivity of the GaN film was observed to be 0.0125 A/W by 365 nm laser. Therefore, the GaN nanofilms prepared by the proposed green and low-cost PECVD method present a strong potential of application in photoelectric devices, such as ultraviolet photodetector, light emitting diodes and epitaxial substrate for the photoelectric materials.

1. Introduction

Gallium nitride (GaN), a direct wide band gap (3.4 eV) semiconductor, is one of the most important semiconductor materials with a wide range of applications in ultraviolet(UV) photodetectors, light emitting diodes, high-speed field-effect transistors and lasers [1–4]. Moreover, GaN can be employed in optoelectronic high-power/high-temperature devices due to reliability and chemical stability [5]. Thus, in recent years, GaN films have attracted a significant research interest for applications in electronic and optoelectronics fields.

Al_2O_3 is a useful substrate material for epitaxial growth of GaN films due to its low-cost, abundant availability, good crystalline quality and lattice match (mismatch ~16 %) [6]. In this respect, Al_2O_3 has been widely used as the substrate material for epitaxial GaN films by employing different synthesis methods [7–13]. For instance, Pant et al. [9] reported the preparation of non-polar GaN films via molecular beam epitaxy (MBE) using Al_2O_3 as substrate. In another study, Yuan et al. [11] obtained GaN films with high crystalline quality by metal-organic chemical vapor deposition (MOCVD). However, the equipments used in these studies are complex and expensive, which limits their widespread use.

To overcome these challenges, extensive research efforts have been made to obtain low-cost GaN films with high quality. For instance, Yang et al. [14] reported that GaN films grown on Al_2O_3 substrate by simple chemical vapor deposition (CVD) using metal gallium and NH_3 as gallium source and nitrogen sources, respectively. Topf et al. [15] reported GaN films grown on Al_2O_3 substrate using $GaCl_3$ and NH_3 as gallium and nitrogen sources, respectively. In a similar study, Nagata et al. [16] reported high quality GaN films prepared by plasma assisted chemical vapor deposition using trimethyl gallium and N_2 as gallium and nitrogen sources. However, the gas sources used in these methods are toxic or corrosive, and the produced GaN films exhibit high defect density, thus, indicating challenges for commercial application.

In this study, high quality GaN nanofilms have been prepared by plasma enhanced chemical vapor deposition (PECVD) using non-toxic raw materials. Specifically, Ga_2O_3 has been used as gallium source, whereas N_2 is employed as nitrogen source. Moreover, the synthesis conditions such as N_2 flow rate, reaction temperature and time have been systematically investigated for analyzing the effect on thickness and evolution of GaN films. Meanwhile, the growth mechanism of GaN films has also been discussed in detail. The proposed green and low-cost method will lead to potential applications in large-scale GaN photoelectric devices such as ultraviolet photodetector as well as epitaxial substrates for photoelectric materials.

* Corresponding author.
E-mail address: wrz@bjut.edu.cn (R.-Z. Wang).

https://doi.org/10.1016/j.tsf.2020.138266
Received 25 February 2020; Received in revised form 2 August 2020; Accepted 3 August 2020
Available online 04 August 2020

Table 1
Growth parameters of all samples

	sample	Temperature (°C)	N_2 flow rate (sccm)	Reaction time (h)
Reaction temperature as variable	1	850	150	2
	2	875	150	2
	3	900	150	2
	4	950	150	2
Reaction atmosphere as variable	5	900	50	2
	6	900	75	2
	7	900	100	2
	8	900	200	2
Reaction time as variable	9	950	150	0.5
	10	950	150	1
	11	950	150	1.5
	12	950	150	2.5

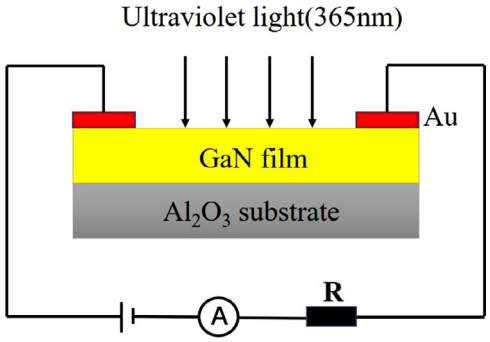

Fig. 1. Schematic diagram of MSM ultraviolet detector

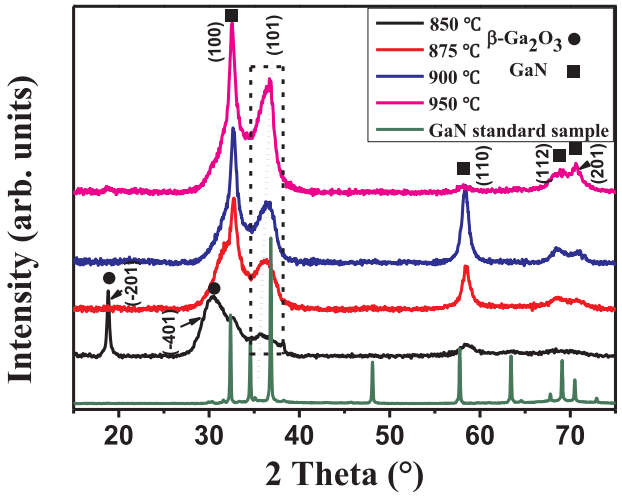

Fig. 2. X-ray diffraction patterns of the products fabricated for different reaction temperatures (reaction time 2 h, N_2 flow rate 150 sccm)

2. Experiment

The GaN films had been prepared on Al_2O_3 substrate by PECVD in a tube furnace using a powder mixture with 1:12 molar ratios of Ga_2O_3 (Alfa, purity 99.999 %) and graphite (purity 99.9 %) as a source material. A sapphire substrate was placed on the top of the source. The furnace was heated at a rate of 20 °C/min under 50 sccm Ar gas (purity 99.999 %). Afterward, N_2 gas (purity 99.999 %) was introduced in the chamber for the growth of GaN film at growth temperature ranging from 850 to 950 °C. The growth was carried out in a nitrogen plasma atmosphere with a N_2 flow rate of 50-200 sccm supplied using a radio frequency (RF) generator working at 100 W for 0.5-2.5 h. After the growth procedure, RF generator was shut off and the sample cooled down to room temperature in pure Ar gas. Finally, a pale-yellow product was found on the substrate. This green, simple, low-cost method to prepare GaN nanofilms on Al_2O_3 substrate was reported. Growth parameters are displayed in Table 1. GaN film (reaction temperature at 950 °C for 2 h, N_2 flow rate 150 sccm) is used as metal-semiconductor-metal (MSM) ultraviolet detector. Au electrodes were deposited in GaN film by sputtering technique. The Au electrode layer is about 75 nm. The length, width and spacing of the interdigital electrode are 600 μm, 150 μm and 200 μm, respectively. The ultraviolet light source is a monochromatic light with the wavelength of 365 nm and the power density of 0.5 mW/cm^2. The schematic diagram of MSM ultraviolet detector is showed in Fig. 1.

A Rigaku Smart lab SE X-ray diffractometer with a Cu Kα_1 radiation in the Bragg Brentano configuration (λ = 0.154178 nm) was used for the Phase identification. The operating voltage is 40 kV. The morphologies of cross-section were observed by field emission scanning electron microscopy (FESEM; Hitachi S4800, 15kV acceleration voltage). The microstructures of film were analyzed by high resolution transmission electron microscopy (HRTEM; Tecnai G20 F20 U-TMIN, 200kV acceleration voltage). HRTEM samples were prepared by focused ion beam (FIB; JEOL JIB-4700F, 20kV acceleration voltage). The morphologies of surface were characterized using atomic force microscopy (AFM, NT-MDT Solver P47) in no-contact mode with 0.5Hz scan rate. The Raman spectra of the samples was investigated by Raman spectroscopy (Raman, Renishaw) with 532 nm laser as an excitation source. The time dependent photoresponsivity of GaN nanofilm detectors was measured by a SourceMeter (KEITHLEY, 2636B system).

3. Results and discussion

3.1. Effect of reaction temperature

Fig. 2 shows the X-ray diffraction patterns of the products fabricated for different reaction temperatures (reaction time 2 h, N_2 flow rate 150 sccm). As shown in Fig. 2, for the reaction temperature of 850 °C, the diffraction peaks at (100), (110), (112) and (201) are identified as the wurtzite-type hexagonal GaN (JCPDS Card No. 50-0792), whereas the diffraction peaks at (-201) and (-401) are identified as the monoclinic β-Ga_2O_3 (JCPDS Card No. 41-1103). As the reaction temperature is increased from 875 °C to 950 °C, the products exhibit the diffraction peaks at (100), (110), (112) and (201) are identified as the wurtzite-type hexagonal GaN. In the dashed box in Fig. 2, the corresponding diffraction angles for the peaks are 35.72 °, 36.15 °, 36.66 °and 36.81 °, respectively. For the reaction temperature of 950 °C, the diffraction peak in the dashed box is observed to be in accordance with (101) plane of the wurtzite-type hexagonal GaN. However, the diffraction angles in the dashed box decreased gradually with increasing the reaction temperature, which can be associated with different oxygen content in these GaN samples [17]. For the reaction temperature of 850 °C, the oxygen content of the sample is relatively high, and the diffraction peaks of the monoclinic β-Ga_2O_3 can be obviously observed in Fig.2. This indicates that the oxygen content in the obtained GaN products can be reduced by enhancing reaction temperature.

Fig. 3 shows that the cross-sectional SEM images of the GaN products fabricated using different reaction temperatures (reaction time 2 h, N_2 flow rate 150 sccm). Uniform GaN films were obtained at different temperatures, as observed in Fig. 3. The films exhibited effective bonding with Al_2O_3 substrate. As the reaction temperature is increased from 850 °C to 950 °C (Fig. 3a–d), the thickness of the prepared GaN films was observed to 1.19, 1.40, 1.78 and 0.48 μm, respectively. For the reaction temperature exceeding 900 °C, the thickness of the obtained GaN films apparently decreased, as GaN decomposes at 1150 K under ambient conditions [18]. The GaN film obtained at 950 °C exhibited the minimum thickness among the films developed using reaction temperatures from 850 °C to 950 °C due to the rapid thermal

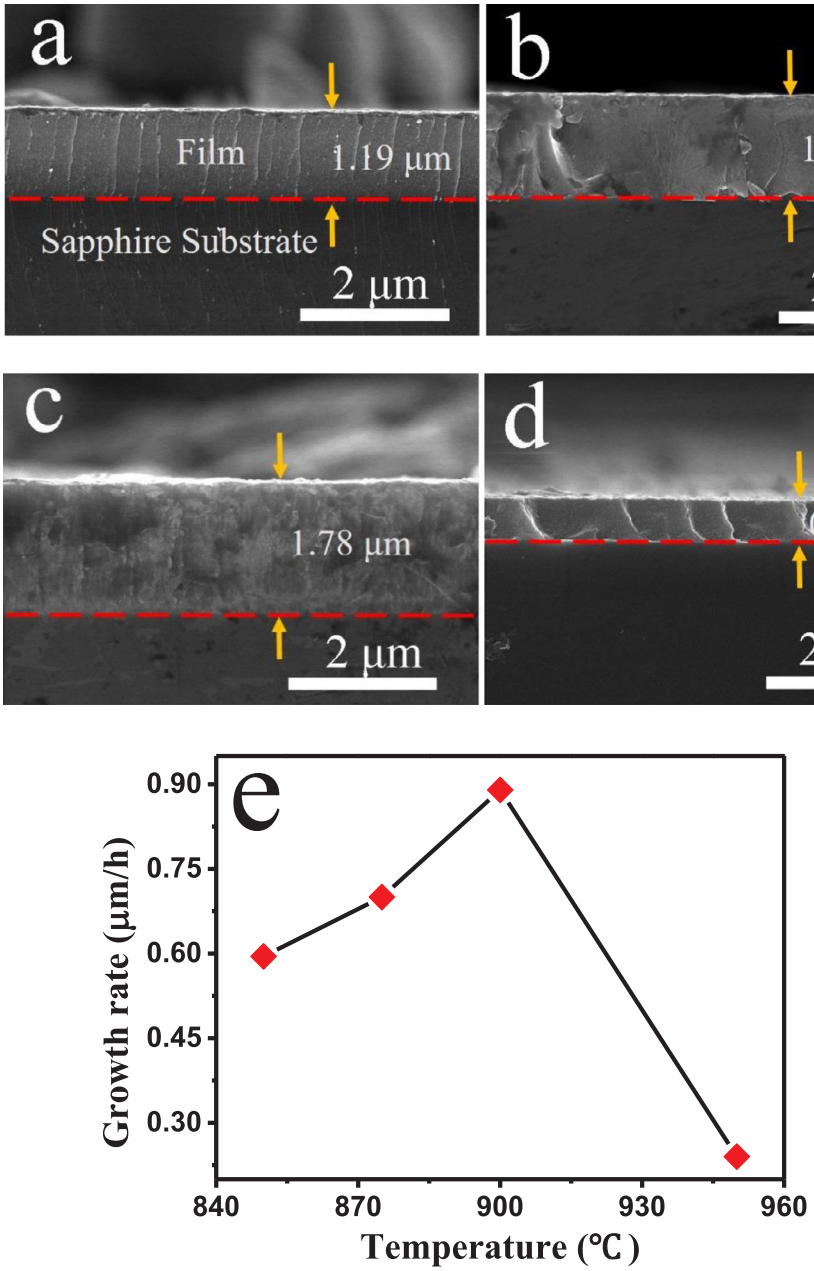

Fig. 3. Cross-sectional SEM images of the GaN products fabricated at different reaction temperatures (reaction time 2 h, N_2 flow rate 150 sccm): (a) at 850 ˚C, (b) at 875 ˚C, (c) at 900 ˚C, and (d) at 950 ˚C; (e) relationship between the growth rate of GaN films and reaction temperature.

decomposition.

The structure as well as optical and electrical properties of GaN film are influenced by the film thickness and mode of growth [19–21] which can be tailored by growth rate of GaN film. The relationship between the growth rate of GaN films and reaction temperature is presented in Fig. 3e. As the reaction temperature increases from 850 ˚C to 900 ˚C, the growth rate of GaN films increases. As the reaction temperature exceeds 900 ˚C, the growth rate of GaN films is subsequently reduced (Fig. 3e). At 950 ˚C, The growth rate of GaN film is observed to be 0.24 μm/h.

Fig. 4 shows the Raman spectra of the GaN film fabricated at 950 ˚C (reaction temperature 2 h, N_2 flow rate 150 sccm). The prominent Raman scattering phonon mode E_2(high), was observed in the GaN sample, which corresponded to the transverse vibration mode of nitrogen atom in wurtzite GaN [22,23]. Apart from the E_2(high) peak, the related Raman spectral peaks of sapphire substrate were also observed at 412, 426, 445, 577, and 748 cm^{-1}. GaN E_2(high) phonon mode is attributed to the nature of the biaxial stress: blue shift of E_2(high) corresponds to the compressive stress whereas red shift discloses the presence of tensile stress in GaN [24]. The E_2(high) phonon peak was observed at 571.8 cm^{-1} for the obtained GaN sample, which indicates the blue shift as compared to stress free GaN (567.6 cm^{-1}). The stress present in the obtained GaN sample is calculated using the following equation [25]:

$$\sigma = \frac{\omega - \omega_0}{4.3} \quad (1)$$

where σ, ω and ω_0 are the biaxial stress, E_2(high) phonon peaks of the obtained GaN films and E_2(high) phonon peak of stress free GaN (567.6 cm^{-1}), respectively. Hence, the calculated compressive stress of the GaN sample is observed to be 0.98 GPa in accordance with the GaN films grown on sapphire substrate by MOCVD or MBE [26,27].

Fig. 5 demonstrates the AFM image of GaN film fabricated for N_2 flow rate 150 sccm at 950 ˚C (reaction time 2 h). The surface of GaN films consisted of numerous nanoislands (Fig. 5), which indicated that

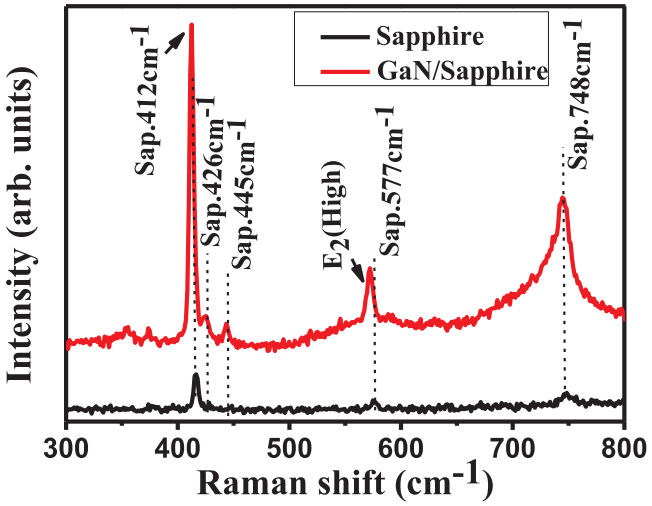

Fig. 4. Raman spectra of GaN film fabricated at 950 °C (at 2 h, N_2 flow rate 150 sccm)

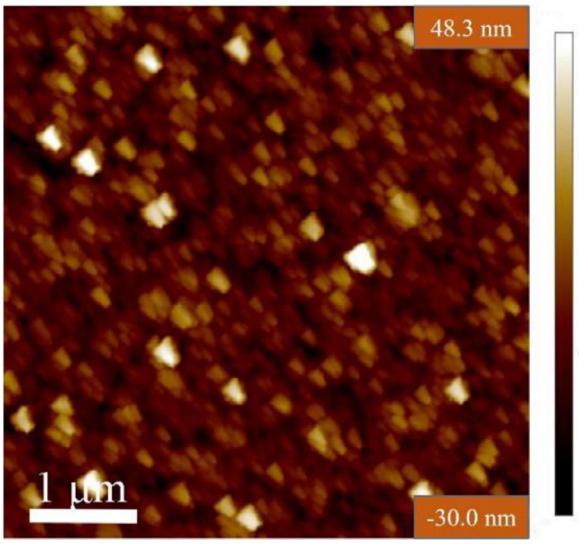

Fig. 5. AFM image of GaN film fabricated for N_2 flow rate 150 sccm at 950 °C (reaction time 2 h).

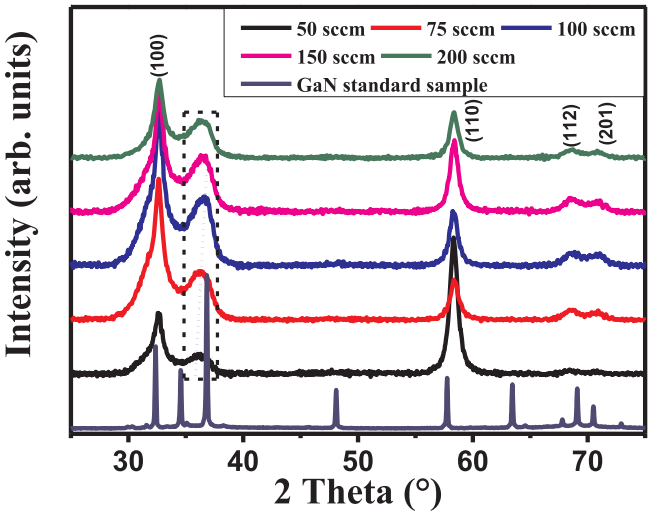

Fig. 6. X-ray diffraction patterns of the products fabricated for different N_2 flow rates (at 900 °C, reaction time 2 h)

the growth mechanism of the GaN films is three-dimensional islands growth mode [26]. In addition, the surface of the GaN films was noted to be flat, with no observed pints (Fig. 5). the roughness Ra of the obtained GaN film was measured to be 7.13 nm.

3.2. Effect of reaction atmosphere

Fig. 6 presents the X-ray diffraction patterns of the products fabricated for different N_2 flow rates (at 900 °C, reaction time 2 h). According to the standard PDF card, the diffraction peaks at (100), (110), (112) and (201) are identified as the wurtzite-type hexagonal GaN (JCPDS Card No. 50-0792) reflected in Fig. 6a. In the dashed box in Fig. 6a, the corresponding diffraction angle for the obtained products are observed at 36.28 °, 36.37 °,36.69 °,36.66 °and 36.37 °, respectively. Hexagonal GaN (101) plane corresponds to peak angle 36.85 °, and β-Ga_2O_3 (111) plane is observed at 35.18 °. Thus, the diffraction peaks of the obtained samples in the dashed box lied between 35.18 ° and 36.85 °. Compared with the hexagonal GaN (101) plane, the diffraction peaks of the obtained GaN samples in the dashed box exhibit angular deviation, which may result from the presence of oxygen in the obtained GaN samples [17]. The angular deviation of the obtained GaN samples was observed to decrease and subsequently increase with increasing the N_2 flow rate. The observed phenomenon indicates that the oxygen content in the obtained GaN samples decreased and subsequently increased with an increase the N_2 flow rate. As N_2 flow rate increased from 50 to 150 sccm, the concentration of the N plasma also increased. It may indicate that the high N plasma concentration hindered the reaction of Ga with oxygen. For the N_2 flow rate of 200 sccm, the high gas flow rate resulted in a barrier to the reaction of Ga with N plasma [11], thus, contributing to the increase in the oxygen content.

Fig. 7 displays the cross-sectional SEM images of the GaN products fabricated for different N_2 flow rates (at 900 °C, reaction time 2 h). Uniform GaN films could be observed in Fig. 7, with effective bonding between the film and Al_2O_3 substrate. As the N_2 flow rate increased from 50 to 200 sccm (Fig. 7a–e), the corresponding thickness of the obtained GaN films are 0.82 μm, 1.16 μm, 1.20 μm, 1.78 μm, and 1.58 μm. Thus, the thickness of the obtained GaN films increases and subsequently decreases with increasing the N_2 flow rate. For the N_2 flow rate of 150 sccm, the thickness of the obtained GaN film was observed to be the maximum with growth rate of 0.89 μm/h. However, for the N_2 flow rate of 200 sccm, the thickness of the obtained GaN film decreases due to high N/Ga ratio. Fig. 7f displays the relationship between the growth rate of GaN films and N_2 flow rate. With an increase in the N_2 flow rate, the growth rate of GaN films increases and subsequently decreases.

Fig. 8 shows AFM images of the GaN films fabricated for different N_2 flow rates (at 900 °C, reaction time 2 h), revealing the flat surface of the GaN films. The roughness Ra of the obtained GaN films (for N_2 flow rates from 50 to 200 sccm) were measured to be 9.45 nm, 7.35 nm, 10.7 nm and 6.81 nm, respectively. As seen in Fig. 8, the surface of the GaN films consisted of numerous nanoislands, which indicated that the three-dimensional island growth mode was the growth mechanism for the GaN films [26]. In addition, no cracks and pins were observed in Fig. 8, thus, suggesting that high quality GaN films could be obtained [28].

3.3. Effect of reaction time

Fig. 9 shows the X-ray diffraction patterns of the products fabricated for different reaction time (at 950 °C, N_2 flow rate 150 sccm). According to the standard PDF card, the diffraction peaks at (100), (110), (112) and (201) indicate the wurtzite-type hexagonal GaN (JCPDS Card No. 50-0792). For the reaction time of 0.5-1.5 h, the diffraction peak of the hexagonal GaN (002) plane could be observed for all GaN samples, and the intensity of (002) plane diffraction peak gradually decreased with increasing the reaction time. For reaction time exceeding 2 h, the

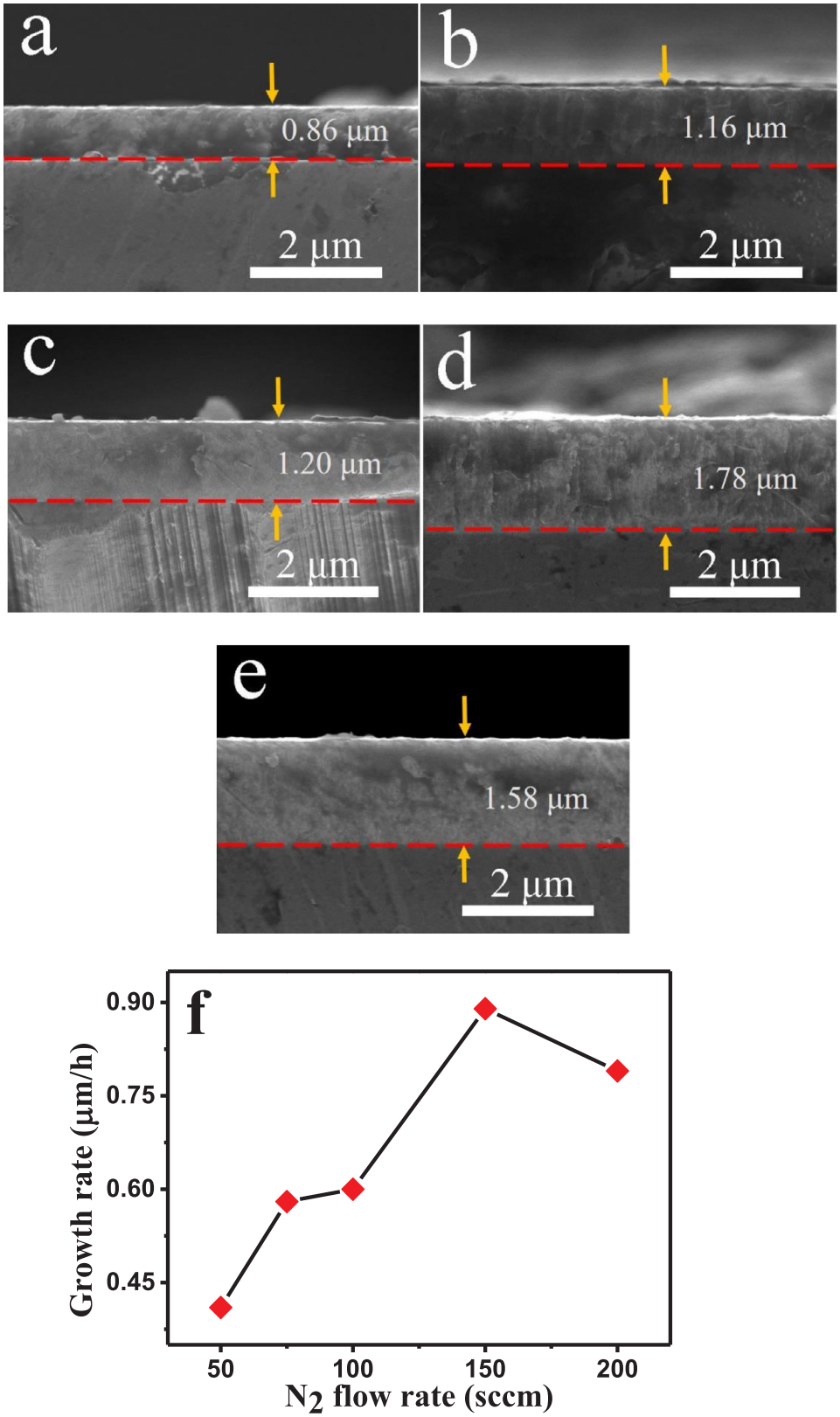

Fig. 7. Cross-sectional SEM images of the GaN products fabricated for different N_2 flow rates (at 900 °C, reaction time 2 h): (a) 50 sccm, (b) 75 sccm, (c) 100 sccm, (d) 150 sccm, (e) 200 sccm; (f) relationship between the growth rate of GaN films and N_2 flow rate.

diffraction peak of the hexagonal GaN (002) plane was absent in the diffractograms of the GaN samples. The observed phenomenon revealed the preferential growth of the materials.

Fig. 10 displays the cross-sectional SEM images of the GaN products fabricated for different reaction time (at 950 °C, N_2 flow rate 150 sccm). As seen in Fig. 10, uniform GaN films were obtained at different reaction time. As the reaction time increased from 0.5 to 2.5 h (Fig. 10a–e), the thickness of the obtained GaN films are 0.07 μm, 0.24 μm, 0.29 μm,

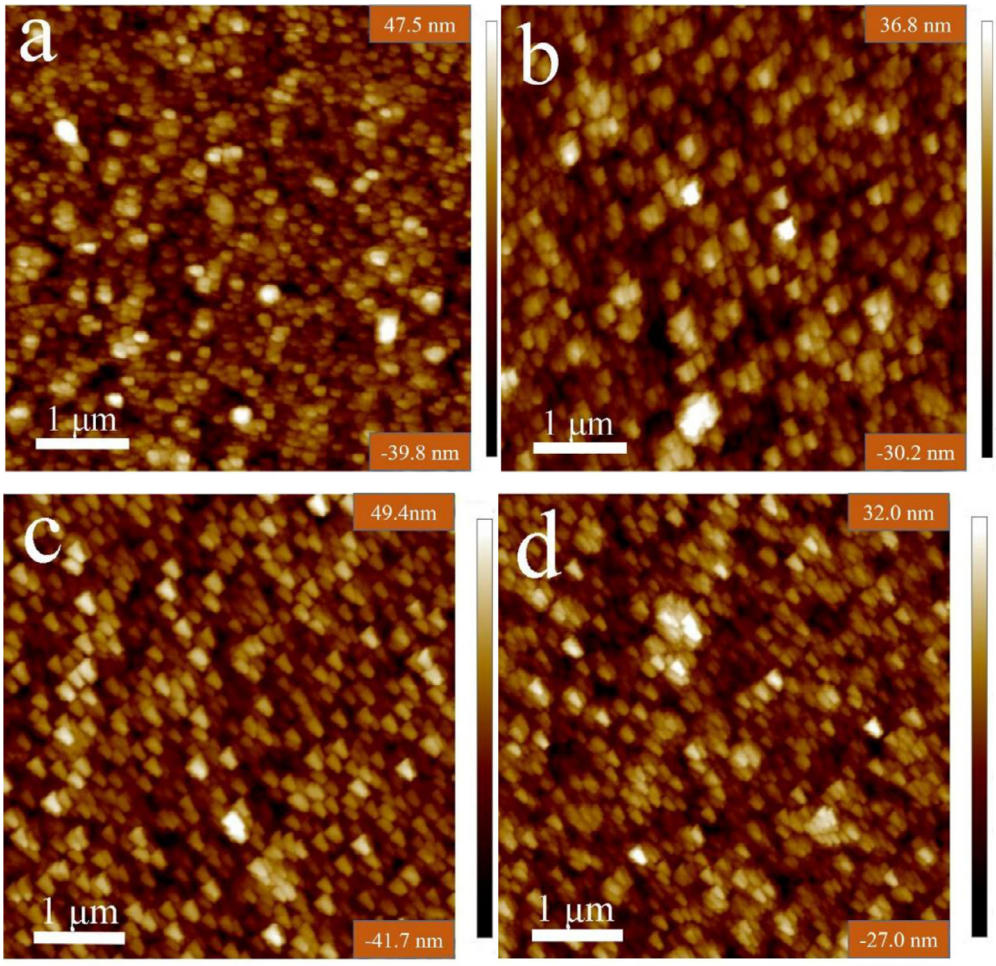

Fig. 8. AFM images of the GaN films fabricated for different N_2 flow rates (at 900 °C, reaction time 2 h): (a) 2D image for 50 sccm, (b) 2D image for 100 sccm, (c) 2D image for 150 sccm, and (d) 2D image for 200 sccm.

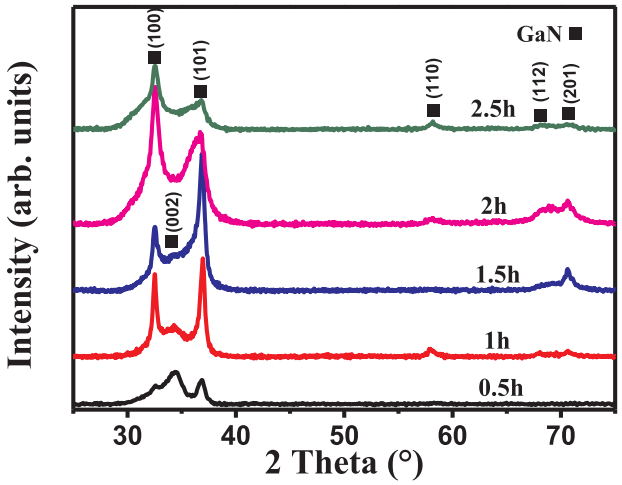

Fig. 9. X-ray diffraction patterns of the products fabricated for different reaction time (at 950 °C, N_2 flow rate 150 sccm).

0.48 μm, and 0.51 μm. Thus, the thickness of the obtained GaN films increases with an increase in the reaction time. However, the growth rate of the GaN film is non-uniform. The growth rate of GaN film for the reaction duration of 0.5 h was observed to be slow (Fig. 10a). The observed phenomenon might have resulted from the nucleation process of GaN film. For reaction time exceeding 0.5 h, the growth rate of GaN film increases. Furthermore, the surface of GaN film was rough for the reaction duration of 1 h. With further enhancing the reaction duration, the surface of GaN films became flat and the growth rate is uniform. As seen from Fig. 10b–d, the growth rate of GaN film is about 0.2 μm/h. The result indicates that the thickness of GaN films can be tailored through the reaction time.

Fig.11a displays that cross-sectional TEM image of GaN film fabricated at 950 °C for 2 h (N_2 flow rate 150 sccm). The corresponding HRTEM and diffraction pattern images for GaN film at area B are shown in Fig.11b. The HRTEM and diffraction pattern images reveals polycrystallinity with hexagonal wurtzite structure in synthesized GaN film. The adjacent spacing of the lattice fringes in the HRTEM image was measured to be 0.28 nm, which corresponds to the (100) plane of the wurtzite GaN [29]. Fig. 11c shows the HRTEM image of the interface between the GaN film and Al_2O_3 substrate. The spacing of the lattice fringes in the HRTEM image is 0.35 nm, corresponding to the (012) plane of the hexagonal Al_2O_3 substrate [30]. The interface exhibits obvious atomic misarrangement, which is contributed to improving crystal quality of GaN film. The interface layer of atomic misarrangement increases the robustness of GaN films [31].

3.4. Growth mechanism

In this study, N_2 was ionized by coupled with the RF in the synthesis process. For the synthesis of crystalline GaN, carbothermal reduction of Ga_2O_3 by graphite occurs first with formation of gaseous Ga_2O and Ga [32–34]; Then, the reaction of gaseous Ga with ionized nitrogen plasma result in the formation of GaN [35]. Therefore, the reactions can be

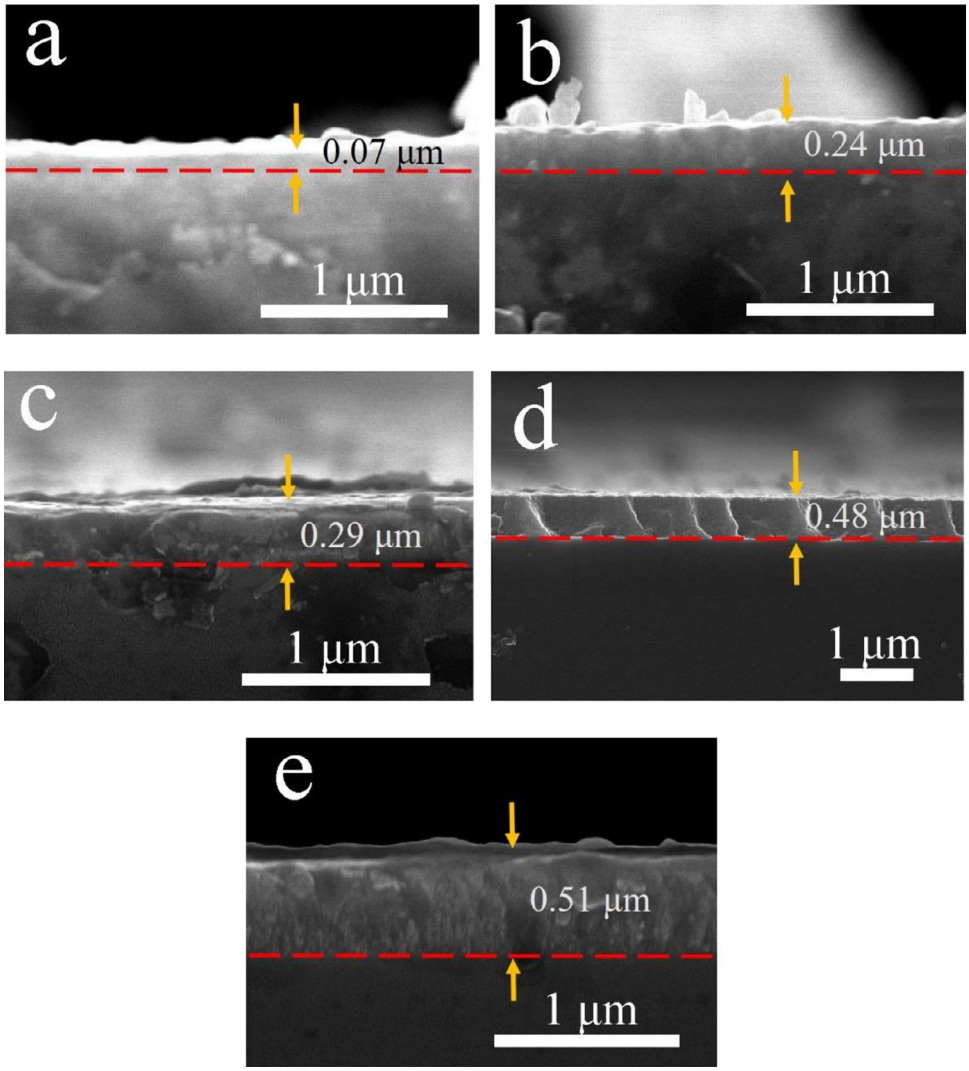

Fig. 10. Cross-sectional SEM images of the GaN products fabricated for different reaction time (at 950 °C, N_2 flow rate 150 sccm): (a) 0.5 h, (b) 1 h, (c) 1.5 h, (d) 2 h, and (e) 2.5 h.

expressed as:

$$N_2(g) \xrightarrow{RF} N^*(g) \quad (2)$$

$$Ga_2O_3(s) + C(s) \rightarrow Ga_2O(g) + CO(g) \quad (3)$$

$$Ga_2O(g) + C(s) \rightarrow Ga(g) + CO(g) \quad (4)$$

$$Ga(g) + N^*(g) \rightarrow GaN(s) \quad (5)$$

For the formation of high quality GaN films by PECVD method, the ionized nitrogen plasma and graphite reductive agent are the vital component. Firstly, NH_3 is used as nitrogen source in the CVD method, and the hydrogen radicals present in the reaction atmosphere get bonded to part of nitrogen to prevent the reaction with gaseous Ga or etching of GaN [36,37]. Thus, it is challenging to obtain uniform and high quality GaN films in the conventional CVD method. The same phenomenon was also observed in current study. With N_2 and H_2 mixed gases used as reaction source, no products were obtained on the substrate. N_2 gas is used as N source in the current study instead of NH_3, thus, no hydrogen radicals are presented in the reaction atmosphere to etch GaN and restrict the deposition of GaN films. Meanwhile, the ionized nitrogen plasma formed by radio frequency exhibited high energy and numerous dangling bonds which enhanced the uniform adsorption at Al_2O_3 substrate and contributed to the reaction with gaseous Ga. Secondly, the reaction of graphite with Ga_2O_3 can form uniform gaseous Ga, which provided optimal reaction atmosphere for the deposition of GaN. Compared to trimethyl gallium, the proposed method in this study can avoid the unfavorable effect of the hydrogen radicals formed by the decomposition of trimethyl gallium. Therefore, graphite, as reductive agent, contributed to the nucleation of GaN and restricted the formation of defects.

The reaction temperature is a key factor affecting the oxygen content of the GaN films. Generally, the reaction 4 occur at high temperature which provided enough energy for the reaction of Ga_2O with graphite to form gaseous Ga. For the reaction temperature below 900 °C, the formation of GaN occurred by the reaction of Ga_2O and Ga with ionized nitrogen plasma. Thus, the obtained GaN films contain oxygen, as observed form Figs. 2 and 6. With an increase in the reaction temperature, the content of oxygen in the GaN films decrease due to a reduction in Ga_2O/Ga ratio in the reaction atmosphere. No oxygen is observed in the high quality GaN film which obtained at 950 °C (Fig. 2).

Moreover, the thickness and growth rate of the GaN films are influenced by the reaction atmosphere and temperature (Figs. 3 and 7). The concentration of the nitrogen plasma increases with increasing N_2 flow rate, which contributes to the growth of GaN films. However, the growth of the GaN films is restricted by high N/Ga ratio which caused by superfluous N_2 gas flow [38]. Although high temperature provides high energy to promote the synthesis and deposition of GaN, it results in the thermal decomposition of GaN. For the reaction temperature of 950

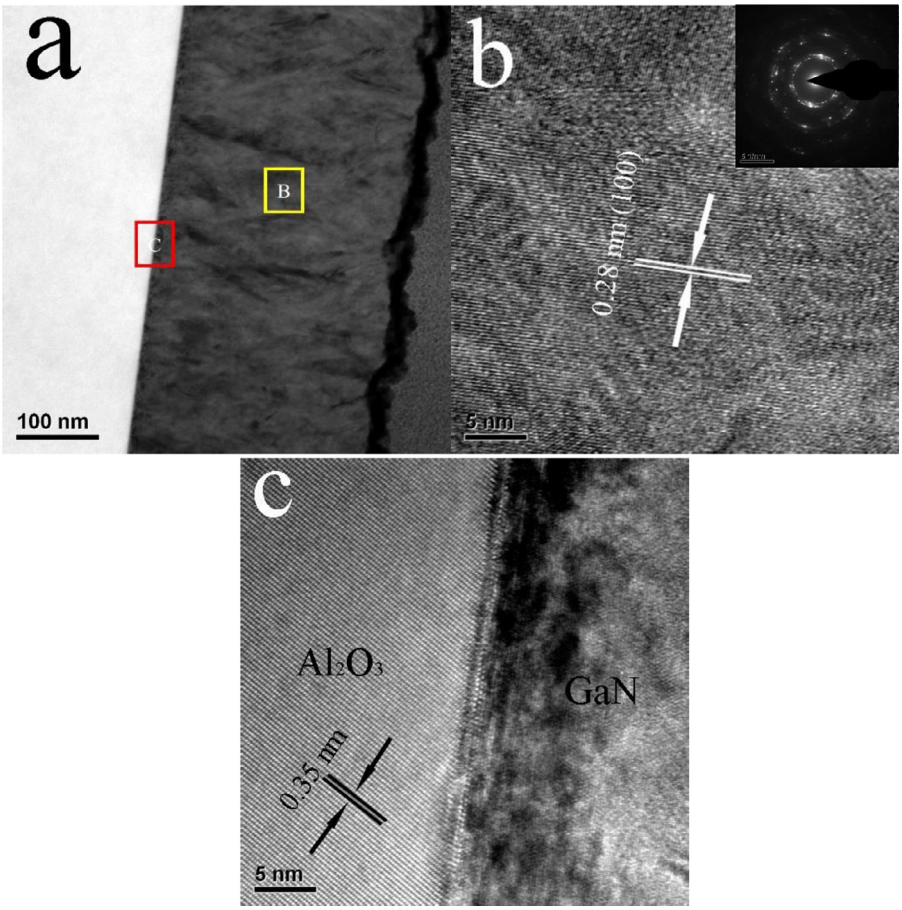

Fig. 11. (a) Cross-sectional TEM image of products fabricated at 950 °C for 2 h (N_2 flow rate 150 sccm). (b) and (c) are HRTEM images at area B and C of Fig. 11(a), respectively.

°C, the thickness and growth rate of GaN films decrease due to the rapid thermal decomposition of GaN exceeding the deposition rate.

3.5. Photoelectric properties

The electrical transport properties of the GaN MSM photodetector were characterized by measuring I-V curve under dark at room temperature as shown in Fig. 12a. the non-linear I-V curve was observed for the GaN detector, which demonstrates that Au electrodes formed Schottky-type contact with GaN. The dark current resulted due to the defects in GaN [39,40]. The dark current value of the GaN detector is noted to be in microampere scale, which indicates that GaN film has a relatively low density of defect. Further, Fig. 12b shows the time dependent UV-light photo responsivity at 5 V bias voltage for the GaN MSM photodetectors fabricated using GaN film (reaction temperature at 950 °C for 2 h, N_2 flow rate 150 sccm). The rise in photocurrent after turning-on the UV light and decay in current after turning-off the light was observed for several cycles, which demonstrates that the photoresponse of GaN detector is stable and repeatable. When the UV light is turned off, the current drops very slowly. Because the deep levels represent the carrier recombination center. The slow current drop observed in Fig. 12b may be caused by the detrapping process of the carriers at deep levels in the wide band gap of materials [41,42]. The calculated photoresponsivity of MSM-GaN detector is 0.0125 A/W under 365 nm UV-light. Other nitride semiconductor ultraviolet photodetectors are also summarized in Table 2.

4. Conclusions

In summary, we have prepared GaN films by green and low-cost PECVD method using non-toxic raw materials. The ionized nitrogen plasma and graphite reductive agent paly vital role for the development of the high-quality GaN films. The ionized nitrogen plasma formed by radio frequency exhibit high energy and numerous dangling bonds which are contributed to enhanced uniform deposition at Al_2O_3 substrate. The reaction of graphite with Ga_2O_3 can form uniform gaseous Ga, which provided uniform reaction atmosphere for the deposition of GaN. Graphite, as reductive agent, which can avoid the hydrogen radicals to etch GaN and restrict the growth of GaN. The AFM indicate that the surface of GaN film are flat and the roughness of GaN films varying from 7 nm to 10 nm. No pit can be observed on the GaN films. When reaction temperature is at 950 °C and N_2 flow rate is 150 sccm, the thickness of GaN film is 0.48 μm, along with high crystallinity and compressive stress 0.98 GPa. In addition, a non-linear I-V curve and photoresponsivity were also observed for the prepared GaN nanofilms. The proposed method presents a green and low-cost technical route for preparing high-quality nanofilms with potential applications in photoelectric devices.

Credit author statements

This manuscript (entitled '**A green, low-cost method to prepare GaN films by plasma enhanced chemical vapor deposition**') is our original work and has not been published nor has it been submitted simultaneously elsewhere. All authors of this paper have checked the manuscript and have agreed to the submission.

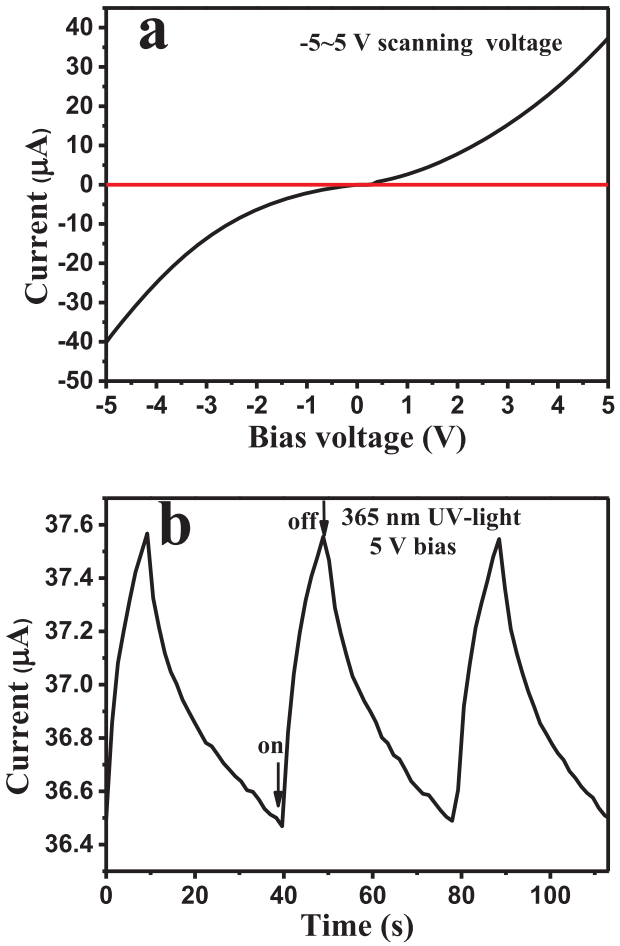

Fig. 12. (a) Typical I-V curve of the GaN MSM device measured under dark at room temperature and (b) time dependent UV-light photo responsivity at 5 V bias voltage for the GaN MSM photodetectors fabricated using GaN film (reaction temperature at 950 °C for 2 h, N_2 flow rate 150 sccm).

Table 2
Parameters of nitride semiconductor ultraviolet photodetectors

Photodetector	UV light (nm)	Bias voltage (V)	Photoresponsivity (A/W)	Reference
$Al_xGa_{1-x}N$	250 – 276	3	0.115	[43]
GaN	365	5	0.05	[44]
AlN	208	50	0.35	[45]
BN	212	20	0.0001	[42]
BN	212	25	0.00133	[46]
GaN	365	5	0.0125	This work

Declaration of Competing Interest

There is no interest conflict with others about publish.

Acknowledgements

This work was financially supported by National Natural Science Foundation of China (Grant Nos. 11774017).

Supplementary materials

Supplementary material associated with this article can be found, in the online version, at doi:10.1016/j.tsf.2020.138266.

References

[1] Y.H. Lin, M.J. Yang, W.L. Wang, Z.T. Lin, G.Q. Li, A low-temperature AlN interlayer to improve the quality of GaN epitaxial films grown on Si substrates, Cryst. Eng. Comm. 18 (2016) 8926–8932, https://doi.org/10.1039/c6ce01974a.
[2] W.L. Wang, Y.L. Zheng, X.C. Li, Y. Li, L.G. Huang, G.Q. Li, High-performance nonpolar a-plane GaN-based metal–semiconductor–metal UV photo-detectors fabricated on $LaAlO_3$ substrates, J. Mater. Chem. C. 6 (2018) 3417–3426, https://doi.org/10.1039/c7tc05534j.
[3] Y. Li, W.L. Wang, X.C. Li, L.G. Huang, Z.T. Lin, Y.L. Zheng, X.F. Chen, G.Q. Li, Stress and dislocation control of GaN epitaxial films grown on Si substrates and their application in high-performance light-emitting diodes, J. Alloys. Compd. 771 (2019) 1000–1008, https://doi.org/10.1016/j.jallcom.2018.09.031.
[4] G.F.A. Malik, M.A. Kharadi, F.A. Khanday, K.A. Shah, Performance analysis of indium phosphide channel based sub-10 nm double gate spin field effect transistor, Phys. Lett. A 384 (2020) 126498, , https://doi.org/10.1016/j.physleta.2020.126498.
[5] N. Takekawa, N. Hayashida, D. Ohzeki, A. Yamaguchi, H. Murakami, Y. Kumagai, K. Matsumoto, A. Koukitu, Growth temperatures and the excess chlorine effect of N-Polar GaN growth via tri-halide vapor phase epitaxy, J. Cryst. Growth. 502 (2018) 7–13, https://doi.org/10.1016/j.jcrysgro.2018.08.024.
[6] Y. Liu, J. Zhang, The effect of coalescence on threading dislocations in GaN films, Scripta. Mater. 63 (2010) 109–112, https://doi.org/10.1016/j.scriptamat.2010.03.025.
[7] M.X. Zhang, Y.Q. Wang, F. Teng, L.L. Chen, J. Li, J.Y. Zhou, X.J. Pan, E.Q. Xie, A photoelectrochemical type self-powered ultraviolet photodetector based on GaN porous films, Mater. Lett. 162 (2016) 117–120, https://doi.org/10.1016/j.matlet.2015.10.001.
[8] W.L. Wang, Z.L. Liu, W.J. Yang, Y.H. Lin, S.Z. Zhou, H.R. Qian, H.Y. Wang, Z.T. Lin, G.Q. Li, Nitridation effect of the α-Al_2O_3 substrates on the quality of the GaN films grown by pulsed laser deposition, RSC Adv. 4 (2014) 39651–39656, https://doi.org/10.1039/c4ra06070a.
[9] R. Pant, A. Shetty, G. Chandan, B. Roul, K.K. Nanda, S.B. Krupanidhi, In-plane anisotropic photoconduction in nonpolar epitaxial a-plane GaN, ACS Appl. Mater. Interfaces 10 (2018) 16918–16923, https://doi.org/10.1021/acsami.8b05032.
[10] C. Ramesh, P. Tyagi, B.S. Yadav, S. Ojha, K.K. Maurya, M.S. Kumar, S.S. Kushvaha, Effect of nitridation temperature on formation and properties of GaN nanowall networks on sapphire (0001) grown by laser MBE, Mater. Sci. Eng. B 231 (2018) 105–114, https://doi.org/10.1016/j.mseb.2018.10.009.
[11] T.T. Yuan, P.Y. Kuei, L.Z. Hsieh, T.C. Li, W.J. Lin, Impact of the gas flow ratio on the physical properties of GaN grown by vertical flow metalorganic chemical vapour deposition, J. Cryst. Growth. 312 (2010) 2239–2242, https://doi.org/10.1016/j.jcrysgro.2010.04.039.
[12] J.P. Mei, X.J. Xie, Q.Y. Hao, W.N. Jing, C.C. Liu, The influence of substrate etched on the quality of GaN epilayers, Appl. Surf. Sci. 257 (2011) 7217–7220, https://doi.org/10.1016/j.apsusc.2011.03.093.
[13] Z.B. Chen, J.C. Zhang, S.R. Xu, J.S. Xue, T. Jiang, Y. Hao, Influence of stacking faults on the quality of GaN films grown on sapphire substrate using a sputtered AlN nucleation layer, Mater. Res. Bull. 89 (2017) 193–196, https://doi.org/10.1016/j.materresbull.2016.12.023.
[14] S.H. Yang, S.H. Ahn, M.S. Jeong, K.S. Nahm, E.K. Suh, K.Y. Lim, Structural and optical properties of GaN films grown by the direct reaction of Ga and NH_3 in a CVD reactor, Solid State Electron. 44 (2000) 1655–1661, https://doi.org/10.1016/S0038-1101(00)00098-8.
[15] M. Topf, S.Fischer G.Steude, W. Kriegseis, I. Dirnstorfer, D. Meister, B.K. Meyer, Low-pressure chemical vapor deposition of GaN epitaxial films, J. Cryst. Growth 189/190 (1998) 330–334, https://doi.org/10.1016/S0022-0248(98)00285-1.
[16] T. Nagata, M. Haemori, Y. Sakuma, T. Chikyow, J. Anzai, T. Uehara, Hydrogen effect on near-atmospheric nitrogen plasma assisted chemical vapor deposition of GaN film growth, J. Appl. Phys. 105 (2009) 066106, , https://doi.org/10.1063/1.3086715.
[17] A. Patsha, S. Amirthapandian, R. Pandian, S. Dhara, Influence of oxygen in architecting large scale nonpolar GaN nanowires, J. Mater. Chem. C. 1 (2013) 8086–8093, https://doi.org/10.1039/c3tc31804d.
[18] R.W. Cumberland, R.G. Blair, C.H. Wallace, T.K. Reynolds, R.B. Kaner, Thermal control of metathesis reactions producing GaN and InN, J. Phys. Chem. B. 105 (2001) 11922–11927, https://doi.org/10.1021/jp0126558.
[19] H. Wang, Y. Huang, Q. Sun, J. Chen, J.J. Zhu, L.L. Wang, Y.T. Wang, H. Yang, M.F. Wu, Y.H. Qu, D.S. Jiang, Depth dependence of structural quality in InN grown by metalorganic chemical vapor deposition, Mater. Lett. 61 (2007) 516–519, https://doi.org/10.1016/j.matlet.2006.05.001.
[20] A. Yamamoto, K. Sugita, H. Takatsuka, A. Hashimoto, V.Y. Davydov, Correlations between electrical and optical properties for OMVPE InN, J. Cryst. Growth. 261 (2004) 275–279, https://doi.org/10.1016/j.jcrysgro.2003.11.082.
[21] H. Lu, W.J. Schaff, J. Hwang, H. Wu, G. Koley, L.F. Eastman, Effect of an AlN buffer layer on the epitaxial growth of InN by molecular-beam epitaxy, Appl. Phys. Lett. 79 (2001) 1489–1491, https://doi.org/10.1063/1.1402649.
[22] V. Purushothaman, V. Ramakrishnan, K. Jeganathan, Interplay of VLS and VS growth mechanism for GaN nanowires by a self-catalytic approach, RSC Adv. 2 (2012) 4802–4806, https://doi.org/10.1039/c2ra01000c.
[23] V. Purushothaman, V. Ramakrishnan, K. Jeganathan, Whiskered GaN nanowires by self-induced VLS approach using chemical vapor deposition, Cryst. Eng. Comm. 14 (2012) 8390–8395, https://doi.org/10.1039/c2ce25770j.
[24] C. Ramesh, P. Tyagi, B. Bhattacharyya, S. Husale, K.K. Maurya, M.S. Kumar, S.S. Kushvaha, Laser molecular beam epitaxy growth of porous GaN nanocolumn

and nanowall network on sapphire (0001) for high responsivity ultraviolet photodetectors, J. Alloys. Compd. 770 (2019) 572–581, https://doi.org/10.1016/j.jallcom.2018.08.149.
[25] Y. Li, W.L. Wang, X.C. Li, L.G. Huang, Z.T. Lin, Y.L. Zheng, X.F. Chen, G.Q. Li, Stress and dislocation control of GaN epitaxial films grown on Si substrates and their application in high-performance light-emitting diodes, J. Alloys. Compd. 771 (2019) 1000–1008, https://doi.org/10.1016/j.jallcom.2018.09.031.
[26] X.T. Liu, D.B. Li, X.J. Sun, Z.M. Li, H. Song, H. Jiang, Y.R. Chen, Stress-induced in situ epitaxial lateral overgrowth of high-quality GaN, Cryst. Eng. Comm. 16 (2014) 8058–8063, https://doi.org/10.1039/c4ce01003e.
[27] S.S. Kushvaha, M.S. Kumar, B.S. Yadav, P.K. Tyagi, S. Ojha, K.K. Maurya, B.P. Singh, Influence of laser repetition rate on the structural and optical properties of GaN layers grown on sapphire (0001) by laser molecular beam epitaxy, Cryst. Eng. Comm. 18 (2016) 744–753, https://doi.org/10.1039/c5ce02257f.
[28] S. Çörekçi, M.K. Öztürk, M. Çakmak, S. Özçelik, E. Özbay, The influence of thickness and ammonia flow rate on the properties of AlN layers, Mat. Sci. Semicon. Proc. 15 (2012) 32–36, https://doi.org/10.1016/j.mssp.2011.06.003.
[29] X.Y. Feng, R.Z. Wang, Q. Liang, Y.H. Ji, M.Q. Yang, Direct growth of GaN nanowires by Ga and N_2 without catalysis, Crys. Growth. Des. 19 (2019) 2687–2694, https://doi.org/10.1021/acs.cgd.8b01817.
[30] H.B. Yang, L. Li, W.B. Cao, Y.H. Liu, M. Mukhtar, L.B. Zhao, Y.M. Kang, Y.H. Dong, J.G. Li, Sintering kinetics and microstructure evolution in α-Al_2O_3 nanocrystalline ceramics: insensitive to Fe impurity, J. Eur. Ceram. Soc. 40 (2020) 1505–1512, https://doi.org/10.1016/j.jeurceramsoc.2019.11.079.
[31] J.I. Hong, Y. Chang, Y. Ding, Z.L. Wang, R.L. Snyder, Growth of GaN films with controlled out-of-plane texture on Si wafers, Thin Solid Films 519 (2011) 3608–3611, https://doi.org/10.1016/j.tsf.2011.01.281.
[32] W.Q. Han, S.S. Fan, Q.Q. Li, Y.D. Hu, Synthesis of gallium nitride nanorods through a carbon nanotube–confined reaction, science 277 (1997) 1287–1289, https://doi.org/10.1126/science.277.5330.1287.
[33] S. Shimada, Y. Miura, A. Miura, Synthesis and characterization of Ge-doped GaN crystalline powders deposited on graphite and silica glass substrates, Cryst. Growth. Des. 7 (2007) 1251–1255, https://doi.org/10.1021/cg068014p.
[34] J.W. Zhao, Y.F. Zhang, Y.H. Li, C.h. Su, X.M. Song, H. Yan, R.Z. Wang, A low cost, green method to synthesize GaN nanowires, Sci. Rep. 5 (2015) 17692, https://doi.org/10.1038/srep17692.
[35] Y.H. Ji, R.Z. Wang, X.Y. Feng, Y.F. Zhang, H. Yan, Modulation effects of hydrogen on structure and photoluminescence of GaN nanowires prepared by plasma-enhanced chemical vapor deposition, J. Phys. Chem. C 121 (2017) 24804–24808, https://doi.org/10.1021/acs.jpcc.7b05532.
[36] J.K. Sprenger, A.S. Cavanagh, H. Sun, K.J. Wahl, A. Roshko, S.M. George, Electron enhanced growth of crystalline gallium nitride thin films at room temperature and 100°C using sequential surface reactions, Chem. Mater. 28 (2016) 5282–5294, https://doi.org/10.1021/acs.chemmater.6b00676.
[37] Y.H. Yeh, K.M. Chen, Y.H. Wu, Y.C. Hsu, W.I. Lee, Hydrogen etching on the surface of GaN for producing patterned structures, J. Cryst. Growth. 314 (2011) 9–12, https://doi.org/10.1016/j.jcrysgro.2010.10.063.
[38] N.L. Liu, Q. Wang, X.P. Zheng, S.F. Li, Y. Dikme, H. Xiong, Y.Z. Pang, G.Y. Zhang, The influence of V/III ratio on GaN grown on patterned sapphire substrate with low temperature AlN buffer layer by hydride vapor phase epitaxy, J. Cryst. Growth. 500 (2018) 85–90, https://doi.org/10.1016/j.jcrysgro.2018.07.014.
[39] X.J. Sun, D.B. Li, H. Jiang, Z.M. Li, H. Song, Y.R. Chen, G.Q. Miao, Improved performance of GaN metal-semiconductor-metal ultraviolet detectors by depositing SiO_2 nanoparticles on a GaN surface, Appl. Phys. Lett. 98 (2011) 121117, , https://doi.org/10.1063/1.3567943.
[40] Y.D. Jhou, S.J. Chang, Y.K. Su, Y.Y. Lee, C.H. Liu, H.C. Lee, GaN Schottky barrier photodetectors with SiN/GaN nucleation layer, Appl. Phys. Lett. 91 (2007) 103506, , https://doi.org/10.1063/1.2779854.
[41] F. Binet, J.Y. Duboz, E. Rosencher, F. Scholz, V. Härle, Mechanisms of recombination in GaN photodetectors, Appl. Phys. Lett. 69 (1996) 1202–1204, https://doi.org/10.1063/1.117411.
[42] H. Liu, J.H. Meng, X.W. Zhang, Y.N. Chen, Z.G. Yin, D.G. Wang, Y. Wang, J.B. You, M.L. Gao, P. Jin, High-performance deep ultraviolet photodetectors based on few-layer hexagonal boron nitride, Nanoscale 10 (2018) 5559–5565, https://doi.org/10.1039/c7nr09438h.
[43] S. Kang, U. Chatterjee, D.Y. Um, Y.T. Yu, I.S. Seo, C.R. Lee, Ultraviolet-C photodetector fabricated using Si-doped n-AlGaN nanorods grown by MOCVD, ACS Photonics 4 (2017) 2595–2603, https://doi.org/10.1021/acsphotonics.7b01047.
[44] C.J. Lee, C.H. Won, J.H. Lee, S.H. Hahm, H. Park, Selectively enhanced UV-A photoresponsivity of a GaN MSM UV photodetector with a step-graded AlxGa1-xN buffer layer, Sensors 17 (2017) 1684, https://doi.org/10.3390/s17071684.
[45] W. Zheng, F. Huang, R.S. Zheng, H.L. Wu, Low-dimensional structure vacuum-ultraviolet-sensitive (λ < 200nm) photodetector with fast-response speed based on high-quality AlN micro/nanowire, Adv. Mater. 27 (2015) 3921–3927, https://doi.org/10.1002/adma.201500268.
[46] M.L. Gao, J.H. Meng, Y.N. Chen, S.Y. Ye, Y. Wang, C.Y. Ding, Y.B. Li. Z.G. Yin, X.B. Zeng, J.B. You, P. Jin, X.W. Zhang, Catalyst-free growth of two-dimensional hexagonal boron nitride few-layers on sapphire for deep ultraviolet photodetectors, J. Mater. Chem. C. 7 (2019) 14999–15006, https://doi.org/10.1039/c9tc05206b.